International Journal of Cardiology xxx (2009) xxx–xxx

Contents lists available at ScienceDirect

International Journal of Cardiology

journal homepage: www.elsevier.com/locate/ijcard

LQTS mutation N1325S in cardiac sodium channel gene *SCN5A* causes cardiomyocyte apoptosis, cardiac fibrosis and contractile dysfunction in mice

Teng Zhang [a,b], Sandro L. Yong [a,b], Jeanne K. Drinko [b], Zoran B. Popović [b], John C. Shryock [c], Luiz Belardinelli [c], Qing Kenneth Wang [a,b,d,*]

[a] *Department of Molecular Cardiology, Lerner Research Institute, Cleveland Clinic, Cleveland, OH, USA*
[b] *Center for Cardiovascular Genetics/NE40, Lerner Research Institute, Cleveland Clinic, 9500 Euclid Avenue, Cleveland, OH 44195, USA*
[c] *Gilead Sciences, Palo Alto, CA, USA*
[d] *Key Laboratory of Molecular Biophysics of Ministry of Education, College of Life Science and Technology, Center for Human Genome Research, Huazhong University of Science and Technology, Wuhan, PR China*

ARTICLE INFO

Article history:
Received 11 June 2009
Received in revised form 17 August 2009
Accepted 21 August 2009
Available online xxxx

Keywords:
Long QT syndrome
Dilated cardiomyopathy
Heart failure
Cardiac sodium channel gene *SCN5A*
Mutation
Cardiomyocyte apoptosis

ABSTRACT

Objective: Mutations in the cardiac sodium channel gene *SCN5A* cause long QT syndrome (LQTS). We previously generated an LQTS mouse model (TG-NS) that overexpresses the LQTS mutation N1325S in *SCN5A*. The TG-NS mice manifested the clinical features of LQTS including spontaneous VT, syncope and sudden death. However, the long-term prognosis of LQTS on the structure of the heart has not been investigated in this or any other LQTS models and human patients.

Methods and results: Impaired systolic function and reduced left ventricular fractional shortening were detected by echocardiography, morphological and histological examination in two lines of adult mutant transgenic mice. Histological and TUNEL analyses of heart sections revealed fibrosis lesions and increased apoptosis in an age-dependent manner. Cardiomyocyte apoptosis was associated with the increased activation of caspases 3 and 9 in TG-NS hearts. Western blot analysis showed a significantly increased expression of the key Ca^{2+} handling proteins L-type Ca^{2+} channel, RYR2 and NCX in TG-NS hearts. Increased apoptosis and an altered expression of Ca^{2+} handling proteins could be detected as early as 3 months of age when echocardiography showed little or no alterations in TG-NS mice.

Conclusions: Our findings revealed for the first time that the LQTS mutation N1325S in *SCN5A* causes cardiac fibrosis and contractile dysfunction in mice, possibly through cellular mechanisms involving aberrant cardiomyocyte apoptosis. Therefore, we provide the experimental evidence supporting the notion that some LQTS patients have an increased risk of structural and functional cardiac damage in a prolonged disease course.

1. Introduction

The *SCN5A* gene, encoding the voltage-gated cardiac sodium channel $Na_v1.5$, is one of the major genes responsible for long QT syndrome (LQTS) [1,2]. The N1325S mutation in *SCN5A* was identified in a 96-member family in which 21 members died suddenly [3]. A follow-up inquiry on the N1325S family discovered that one of the three family members with echocardiographic data showed structural abnormalities consistent with dilated cardiomyopathy (DCM) [3]. This observation prompted us to investigate the long-term prognosis of LQTS in a transgenic mouse model that overexpresses the N1325S mutation (referred to herein as TG-NS mice).

Two lines of TG-NS mice (TG-NSL3 and TG-NSL12 with 1–2 and 10 copies, respectively, of the mutant *SCN5A* with N1325S) and two lines of mice expressing the wild-type *SCN5A* (TG-WTL5 and TG-WTL10 with 1–2 and 10 copies, respectively, of the wild-type *SCN5A*) were generated [4–6]. TG-NSL3 and TG-NSL12 mice showed increases of QTc by 23 and 91%, and increases of action potential duration (APD) by 53 and 128% , respectively, relative to control mice [4]. APD became unstable and markedly prolonged with increasing frequency of stimulation in TG-NS mice [4]. AP alternans, early and delayed after-depolarizations (EADs and DADs, respectively) were detected at decreasing diastolic intervals in TG-NS but not in control mice [3,4]. Compared to TG-WT and non-transgenic (NT) control mice, TG-NS mice showed increased frequencies of ventricular tachycardia (VT), ventricular fibrillation (VF), syncope or sudden death [4,5]. In the current study, we carried out a long-term follow-up investigation of TG-NS mice, using TG-WT mice as age-matched controls [6]. We characterized TG-NS mice for cardiac morphology and contractile

* Corresponding author. Center for Cardiovascular Genetics/NE40, Lerner Research Institute, Cleveland Clinic, 9500 Euclid Avenue, Cleveland, OH 44195, USA. Tel.: +1 216 445 0570; fax: +1 216 636 1231.
E-mail address: wangq2@ccf.org (Q.K. Wang).

0167-5273/$ – see front matter © 2009 Elsevier Ireland Ltd. All rights reserved.
doi:10.1016/j.ijcard.2009.08.047

function, cardiomyocyte apoptosis, fibrosis, activation of caspases, and remodeled expression of key Ca^{2+} handling proteins.

2. Materials and methods

2.1. Experimental animals

Generation and genotyping of TG-NS and TG-WT transgenic mice have been described previously [4,6]. All mice are on a CBA/B6 background. Experimental procedures performed in this study were approved by the Cleveland Clinic Institutional Animal Care and Use Committee, and conform with the NIH Guidelines.

2.2. Morphological and histological analysis

Mice were euthanized by CO_2, and lungs and hearts were isolated immediately. The lung–body weight ratio and heart–body weight ratio were determined by immediate weighing. The whole heart morphology was examined under a dissection microscope (LEICA MZFLIII) at the same magnification. Then, the hearts were washed by PBS and fixed in 4% paraformaldehyde and paraffin-embedded. Serial sections of 10 μm were cut and stained with haematoxylin/eosin (H&E) or Masson's trichrome. All sections were prepared in an identical manner. The presence of interstitial collagen fiber accumulation was used as a marker of cardiac fibrosis. The percentage of interstitial fibrosis to the total heart section area was calculated from 10 randomly selected microscopic fields in four individual sections per heart using ImagePro Plus software (Media Cybernetics, Inc., Bethesda MD).

2.3. TUNEL assays

Frozen sections of heart tissues were used for the TUNEL assay with an ApopTag Peroxidase In Situ Apoptosis Detection Kit (CHEMICON) according to the manufacturer's instructions. Twenty microscopic fields were randomly selected from each section and six individual sections per heart were examined at a high magnification (400×). For each line of mice, 6–17 mice were studied ($n = 6$–17). For each mouse, 5000 to 8000 cells were counted. The number of TUNEL-positive cells and the number of total nuclei were counted, and the percentage was calculated as described [7].

Adjacent heart sections were also examined by double staining of H&E and TUNEL. TUNEL staining was performed as described above except that H&E staining, instead of methyl green above, was used for counterstaining.

2.4. Immunohistochemistry

Frozen heart sections were first stained with TUNEL as described above, and then subjected to a second immunohistochemistry with VECTASTAIN ABC-AP system (Vector Laboratories) with a monoclonal anti-α-actinin antibody (diluted at 1:500, Sigma). The sections were then stained with a biotinylated secondary antibody, and visualized with Vector Red alkaline phosphatase substrate. The sections were counterstained by methyl green.

2.5. Echocardiography

High-frame rate (>200 fps) echocardiography was performed as described [8] with a 14-MHz transducer coupled to an Applio ultrasound machine (Toshiba, Japan).

2.6. Assays for activation of caspases

Caspase-3 activation activity in myocardial tissues was measured with the Caspase-3 Colorimetric Activity Assay Kit according to the instructions by the manufacturer (Chemicon). Caspase-8 and caspase-9 activation activity in myocardial tissues was measured using the Caspase-8 and -9 Colorimetric Assay Kit according to the instructions by the manufacturer (R&D Systems). The assay was performed in triplicate in 96-well plates.

2.7. Western blot analysis

Total protein extracts were extracted from fresh, isolated hearts by using the lysis buffer containing 20 mM Tris–HCl (pH 8.0), 100 mM NaCl, 1 mM EDTA, 0.5% NP-40 and 1× protease inhibitor cocktail solution. Western blot analysis was performed with 30–75 μg of total protein extracts using primary antibodies against Na^+/Ca^{2+} exchanger NCX-1 (Chemicon), SERCA2 (Santa Cruz Biotechnology), dihydropyridine receptor alpha 2 (Bioreagents) and ryanodine receptor RyR2 (Sigma) as well as GAPDH as the loading control.

2.8. Statistical analysis

All values are presented as mean ± SEM. Statistical analysis for group data was performed using one way ANOVA. The paired Student's *t*-test was used to determine the significant level of a difference between two variables. The significance level was set at a P value of less than 0.05 or wherever indicated in the figure legends.

3. Results

3.1. Morphological and histological evidence of abnormal cardiac structure in TG-NS mice

Gross morphological examinations of whole hearts and transverse heart sections from TG-NS mice detected myocardial fibrosis and increased chamber dimensions compared to TG-WTL10 control mice. Enlarged and dilated hearts were seen consistently in both lines of TG-NS mice (TG-NSL3 and TG-NSL12) at 6–10 months of age, but not in comparable control TG-WTL10 and NT mice (Fig. 1). Typical features of DCM were detected in 3 of 6 TG-NSL12 mice and 3 of 9 TG-NSL3 mice by histological examinations and echocardiography described below. Dilatation or enlargement of the heart was rarely detected in

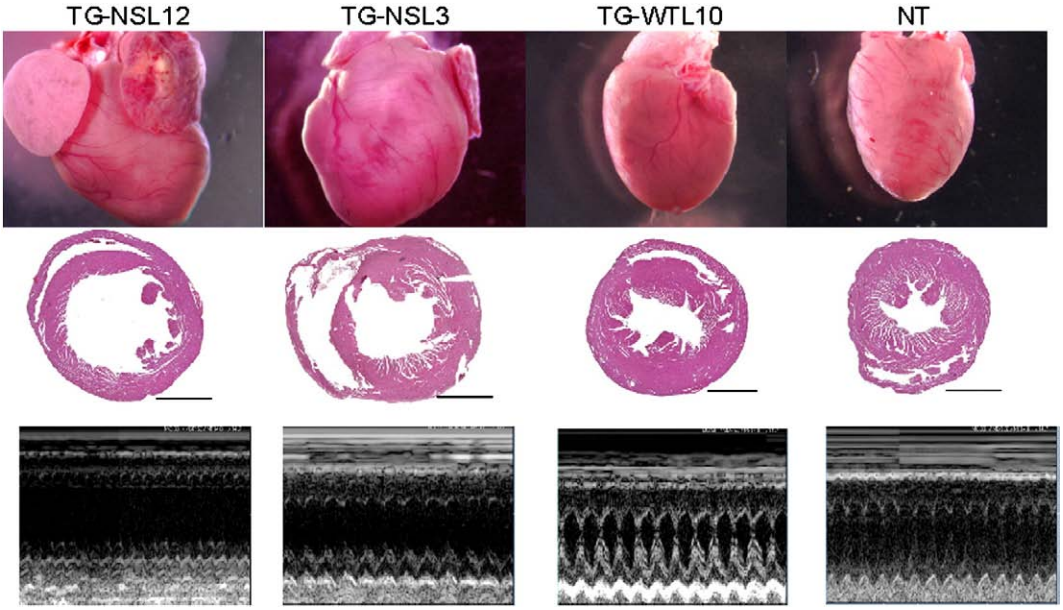

Fig. 1. Abnormal cardiac structure in TG-NS mice. The gross morphology of the whole heart (first row) and H&E staining of transverse heart sections (second row; horizontal bars indicate 200 μm) revealed cardiac enlargement and ventricular dilatation in 6–10-month old TG-NSL12 and TG-NSL3, but not in TG-WTL10 or NT mice. Representative echocardiographic M-mode images for each of the corresponding hearts are illustrated in the third row.

Please cite this article as: Zhang T, et al, LQTS mutation N1325S in cardiac sodium channel gene *SCN5A* causes cardiomyocyte apoptosis, cardiac fibrosis and contractile dysfunction in mice, Int J Cardiol (2009), doi:10.1016/j.ijcard.2009.08.047

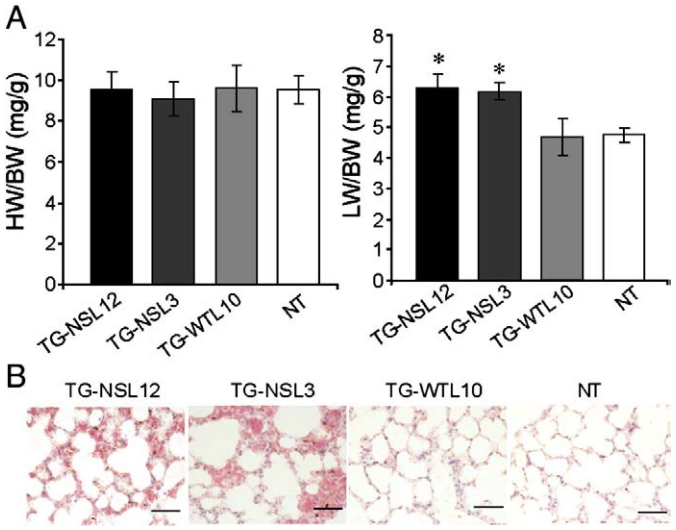

Fig. 2. Histological analysis of the lung. (A) Significant increases in the lung weight/body weight ratio were observed in both lines of TG-NS mice (TG-NS-L12, $n=12$; TG-NS-L3, $n=11$), compared with TG-WTL10 ($n=10$) or NT ($n=19$) mice (*$P<0.01$). The heart/body weight ratios of 6–10-month old TG-NSL12, TG-NSL3, TG-WTL10, and NT mice were not different. (B) Pulmonary congestion and edema were observed in both lines of TG-NS mice at 6–10 months of age. The alveolar capillaries of the lung were distended and filled with erythrocytes. In some areas, the alveolar space was filled with fluids. Normal alveolar structures were shown as in TG-WTL10 or NT mice. $n=3$; scale bar (bottom right panel) = 20 μm.

TG-NS mice at the age of 2–3 months (data not shown). There were no significant differences in values of the heart weight/body weight ratio among TG-NS, TG-WTL10 and NT mice (Fig. 2A, left panel). However, the lung weight/body weight ratio, an index of pulmonary congestion and left ventricular systolic dysfunction, was significantly increased in TG-NS mice compared with NT mice or TG-WTL10 mice (Fig. 2A, right panel). Histological analysis showed pulmonary congestion and edema in TG-NSL3 and TG-NSL12 mice at the age of 6–10 months (Fig. 2B). No significant alteration in a liver/body weight ratio and hepatic congestion was detected in the two lines of TG-NS mice.

Masson's trichrome staining of heart sections from 4 groups of mice at 6–10 months of age showed a significant increase of development of cardiac fibrosis in both lines of TG-NS mice compared with NT and TG-WTL10 mice, respectively (Fig. 3). For mice at the age of 2–3 months, fibrosis was barely detectable and no significant differences were found among the TG-NSL12, TG-NSL3, TG-WTL10, and NT mice (data not shown). Therefore, the morphological and histological alterations in TG-NS mice are indicative of an age-dependent development of contractile dysfunction and myocardial fibrosis.

3.2. Abnormal cardiac structure and functional performance in TG-NS mice by echocardiography

To further explore the phenotype of TG-NS mice, echocardiography was carried out to examine the structural and functional performance of the heart. A significant increase in systolic left ventricular end dimension (LVEDS), and decreases in systolic intraventricular septal thickness (IVSS) and systolic posterior wall thickness (PWS) in 6–10 month TG-NS mice relative to NT or TG-WTL10 mice were noted (Fig. 1 bottom panels, and Table 1). Left ventricular fractional shortening (LVFS) was significantly less in TG-NS mice than in NT mice: values of LVFS in TG-NSL12, TG-NSL3, and NT mice were 24.85 ± 5.64, 42.78 ± 1.95, and $60.0\pm5.7\%$, respectively ($P<0.005$ and $P<0.05$ for TG lines 12 and 3 vs. NT mice; Table 1). TG-WTL10L10 mice displayed normal values of structural parameters (Fig. 1 and Table 1) and a normal LVFS value of $58.44\pm1.80\%$ ($P>0.05$ compared to NT mice), and there were no significant differences between the two TG-WTL10L10 lines with different copy numbers of the transgene (data not shown). Reduced LVFS in TG-NS hearts indicates left ventricular systolic dysfunction. It is interesting to note that the value of LVFS in hearts from TG-NSL12 mice decreased from $42.31\pm0.8\%$ at 3 months to $24.85\pm5.64\%$ at 8 months (Table 1). Similarly, age-dependent alterations in heart structure, as reflected by larger values of LVEDS and LVEDD in 8-month than in 3-month old TG-NSL12 mice (Table 1), were also observed. These data suggest that the development of contractile dysfunction in TG-NSL12 mice was progressive.

The heart rate did not vary significantly in young mice (3 months old) among different groups (Table 1). In 8-month old mice, the heart rate in TG-NSL3 mice did not vary significantly from control mice, however, the rate in TG-NSL12 mice was increased significantly compared to control mice.

3.3. Progressive loss of cardiomyocytes by apoptosis in TG-NS mice

Contractile impairment observed in TG-NS mice prompted us to conduct further studies to investigate the underlying mechanisms. Apoptosis has been recognized as playing an important role in DCM and heart failure [9]. We performed TUNEL assays on cross-sections of TG-NS hearts to detect apoptosis. H&E counterstaining was carried out in conjunction with the TUNEL assay (Fig. 4A-iii, 4A-iv) to identify the apoptotic cells by histology and morphology. Moreover, a typical morphological feature of apoptosis, condensation of nuclear chromatin, was captured in sections from TG-NS heart (Fig. 4A-v), which

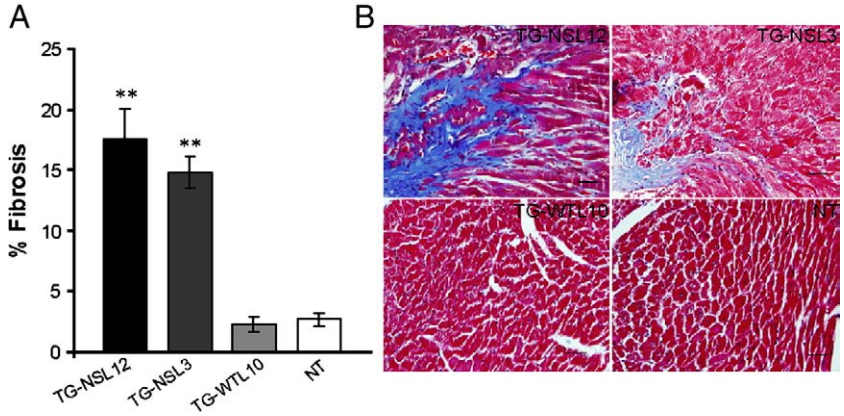

Fig. 3. Significant increase of development of cardiac fibrosis in both lines of TG-NS mice. (A) Representative stained sections from 4 groups of mice ($n=5$ mice/group) indicate fibrosis (light blue color) in both lines of TG-NS mice, but not in TG-WTL10 and NT mice. (B) Fibrotic tissue was greater in 6–10-month old TG-L12 and TG-L3 mice than in TG-WTL10 or NT mice (bar graph), by Masson's trichrome staining of heart sections. Scale bar (bottom right panel) = 20 μm. **Denotes statistically significant difference from TG-WTL10 ($P<0.0001$). (For interpretation of the references to color in this figure legend, the reader is referred to the web version of this article.)

Please cite this article as: Zhang T, et al, LQTS mutation N1325S in cardiac sodium channel gene *SCN5A* causes cardiomyocyte apoptosis, cardiac fibrosis and contractile dysfunction in mice, Int J Cardiol (2009), doi:10.1016/j.ijcard.2009.08.047

Table 1
Echocardiographic assessment of cardiac structure and function in the mice.

Parameters	8 month old mice				3 month old mice		
	TG-NSL12 (6)	TG-NSL3 (9)	TG-WTL10 (6)	NT (9)	TG-NSL12 (7)	TG-NSL3 (5)	NT (10)
LV FS (%)	24.9 ± 5.6**#†	42.78 ± 1.95*	58.44 ± 1.80	59.56 ± 3.88	42.3 ± 1.3**	45 ± 5.52*	63.2 ± 3.62
IVSD (mm)	0.94 ± 0.08	1.08 ± 0.08	0.91 ± 0.10	1.08 ± 0.07	0.98 ± 0.03	1.03 ± 0.06	0.95 ± 0.04
IVSS (mm)	1.25 ± 0.18*	1.67 ± 0.10	1.73 ± 0.10	1.83 ± 0.08	1.57 ± 0.07	1.64 ± 0.04	1.7 ± 0.09
LVEDD (mm)	4.14 ± 0.31#	3.33 ± 0.18	3.76 ± 0.17	3.32 ± 0.15	3.07 ± 0.07	3.35 ± 0.32	2.84 ± 0.14
LVEDS (mm)	3.14 ± 0.37*#†	2.04 ± 0.10*	1.56 ± 0.11	1.41 ± 0.18	1.8 ± 0.04**	1.91 ± 0.35	1.07 ± 0.13
LVPWD (mm)	0.96 ± 0.06	1.02 ± 0.05	0.99 ± 0.10	1.03 ± 0.09	0.90 ± 0.07	0.86 ± 0.04	0.91 ± 0.07
LVPWS (mm)	1.28 ± 0.11*	1.34 ± 0.05*	1.62 ± 0.13	1.61 ± 0.08	1.32 ± 0.08*	1.28 ± 0.12	1.53 ± 0.05
HR (bpm)	812 ± 37.7*†	645 ± 37.3	536 ± 36.5	643 ± 46.3	758 ± 57.1	745 ± 53.7	709 ± 28.2

There were no significant differences between the two TG-WT lines with different copy numbers of the transgene, thus the data are shown for TG-WT L10 only. As in the 8 month old mice, there was no significant difference between TG-WT and NT in the 3 month old mice, thus the data are shown for the NT group only. LVFS—left ventricular fractional shortening, percent change in left ventricular cavity dimensions with systolic contraction ([(LVEDD − LVESD) / LVEDD] × 100); IVSD — left ventricular septal wall thickness in diastole; IVSS—left ventricular septal wall thickness in systole; LVEDD—left ventricular cavity size in diastole; LVEDS—left ventricular cavity size in systole; LVPWD—left ventricular posterior wall thickness in diastole; LVPWS— left ventricular posterior wall thickness in systole; HR—heart rate (bpm—beats per minute); TG-NSL12—mutant transgenic line L12; TG-NSL3—mutant transgenic line L3; TG-WTL10—transgenic mice with wide type *SCN5A* (line 10); NT—non-transgenic mice. The number of mice used for each group is in the bracket after each mouse line; compared with NT, $^{**}P<0.005$, $^{*}P<0.05$; compared with 3-month old group, $^{\#}P<0.05$; compared with TG-NSL3, $^{\dagger}P<0.05$.

further supports apoptotic development [10]. A higher percentage of TUNEL-positive nuclei was found in TG-NS hearts than in control hearts (Fig. 4A-i, 4A-ii, 4B). The percentage of TUNEL-positive nuclei was 2.83 ± 0.28% in TG-NSL12, 2.13 ± 0.53% in TG-NSL3, 0.06 ± 0.02% in TG-WTL10 and 0.07 ± 0.01% in NT hearts at the age of 6–10 months (Fig. 4B). Immunohistochemical analysis using a cardiomyocyte-specific anti-α-actinin antibody in conjunction with the TUNEL assay verified that the TUNEL-positive cells were indeed cardiomyocytes (Fig. 4A-vi). Further analyses showed that cardiomyocyte apoptosis (i.e., the percentage of TUNEL-positive cells) increased with age in TG-NSL12 hearts from 0.21% in 3-month old mice to 3.90% at the age of more than 10 months (Fig. 4C).

3.4. Increased activation of caspase-3 and 9 associated with cardiomyocyte apoptosis

As apoptosis is usually mediated by activation of caspases [7], we next examined the state of activation of caspases 3, 8, and 9 in TG-NS hearts. Caspase-3 activity was nearly 60% greater in TG-NSL12 than in TG-WTL10 or NT hearts (Fig. 5A). Further analysis revealed a significant

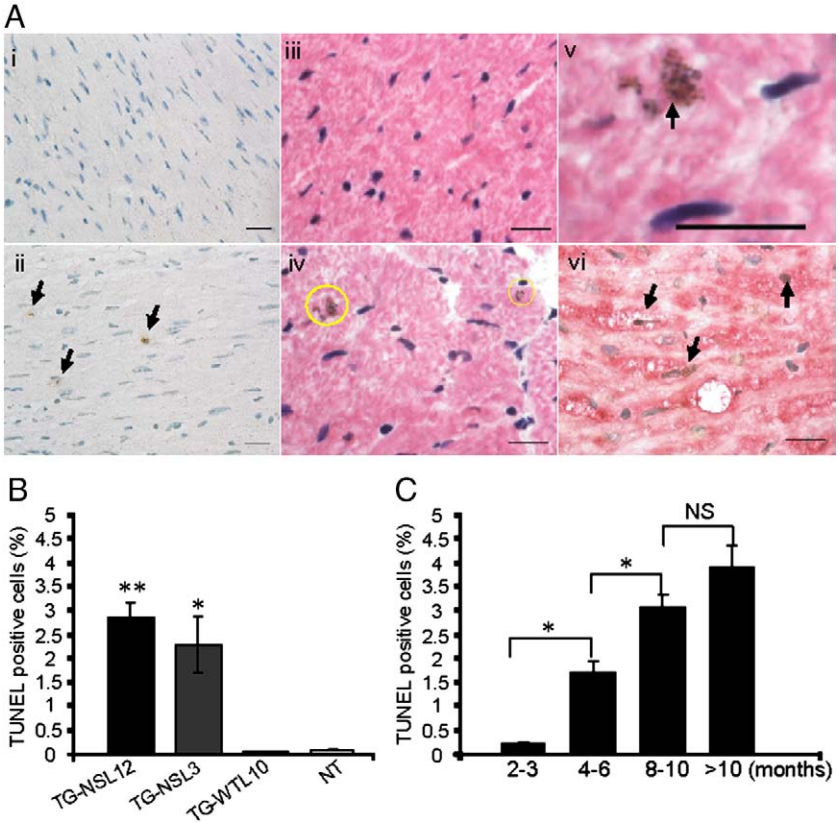

Fig. 4. Evaluation of cardiomyocyte apoptosis. (A) Representative images of heart sections using the TUNEL assay. Brown nuclei are TUNEL-positive and apoptotic cells (arrows). i, NT; ii, TG-NSL12; iii and iv, TUNEL stained images counterstained with H&E for NT and TG-NSL12, respectively; v, a representative image of a TUNEL-positive nucleus undergoing condensation of nuclear chromatin (arrow); vi, image of TG-NSL12 with staining for both TUNEL and a monoclonal anti-α-actinin antibody, a probe specific for cardiomyocytes. Scale bar = 20 μm. (B) The fraction of TUNEL-positive nuclei in hearts of 6–10-month old TG-NSL12 ($n=10$) and TG-NSL3 ($n=6$) mice was significantly greater than in hearts of TG-WTL10 ($n=10$), and NT ($n=17$) mice. ($^{**}P<0.0001$ vs. TG-WT; $^{*}P<0.05$ vs. NT). (C) The number of TUNEL-positive nuclei in hearts of TG-NSL12 mice increased with age. ($^{*}P<0.05$; NS means no significant difference; $n=4$ for 2–3 months, $n=6$ for 4–6 months, $n=6$ for 8–10 months, $n=5$ for more than 10 months group).

Please cite this article as: Zhang T, et al, LQTS mutation N1325S in cardiac sodium channel gene *SCN5A* causes cardiomyocyte apoptosis, cardiac fibrosis and contractile dysfunction in mice, Int J Cardiol (2009), doi:10.1016/j.ijcard.2009.08.047

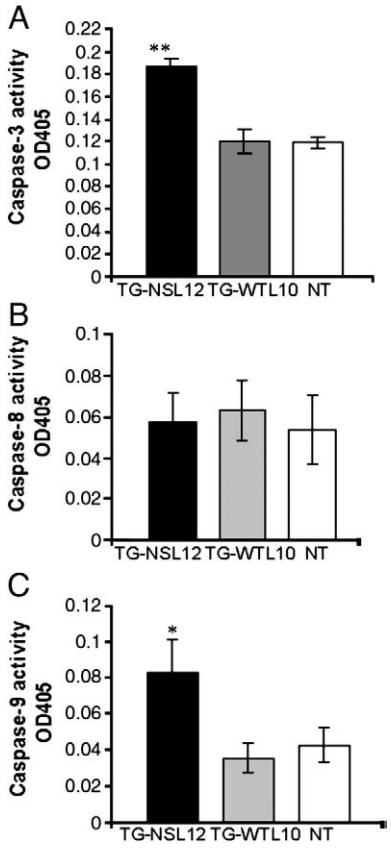

Fig. 5. Assessment of caspase activation in heart tissue. (A) Increased caspase-3 activation was detected in hearts from TG-NSL12 ($n=17$) compared to those from TG-WTL10 ($n=9$) and NT ($n=17$) mice. $^{**}P=2.6\times10^{-9}$ vs. NT. (B) No significant difference was detected in caspase-8 activation amongst the three heart groups. (C) Increased caspase-9 activation was detected in TG-NSL12 hearts ($n=10$) compared to TG-WTL10 ($n=12$) and NT ($n=11$). Age, 3–5 months old; $^{*}P<0.05$ vs. NT.

2-fold increase in caspase-9 (Fig. 5C), but no change in caspase-8 activity (Fig. 5B) in TG-NSL12 hearts compared with controls. These data suggest that apoptosis in TG-NS hearts may involve the caspase-9-dependent mitochondrial apoptotic pathway.

3.5. Alterations of Ca^{2+} handling proteins in TG-NS mice

Remodeling of expression of some key Ca^{2+} handling proteins was evaluated in TG-NS and control mice (Fig. 6). Significantly increased expression of NCX-1, RyR2 and L-type Ca^{2+} channel was detected in both lines of TG-NS mice compared to TG-WTL10 and NT mice (Fig. 6A, B, D). However, the expression of SERCA2 was not significantly different amongst the 4 groups of mice (Fig. 6C).

4. Discussion

The N1325S mutation in the cardiac sodium channel gene *SCN5A* has been previously shown to cause type-3 LQTS (LQT3) in both humans and mice. The results from this study clearly demonstrate that mutation N1325S also causes myocardial damage in a progressive, age-dependent manner. Echocardiographic and histological examinations of hearts from the TG-NS mice with N1325S revealed structural and functional impairment of the left ventricle, and findings reminiscent of abnormalities seen in human heart failure patients, which were not detected in age-matched control TG-WTL10 mice overexpressing wild-type *SCN5A*. The lung weight/body weight ratio in TG-NS mice was greater than in control mice. Pulmonary congestion and edema were observed in both lines of TG-NS mice. The increased ratio may reflect the presence of lung edema secondary to left ventricular dysfunction [11].

The observed phenotype in TG-NS mice is unlikely to be caused by excessive overexpression of *SCN5A*. Transgenic TG-NSL12 mice expressing the mutant N1325S *SCN5A* gene and transgenic TG-WTL10 mice expressing the wild-type gene have the same copy number and expression level of the transgene, but only the former developed the heart failure phenotype. Secondly, TG-NSL3 mice, which express 1–2 copies of the mutant transgene, also developed the same DCM and heart failure phenotype as TG-NSL12, albeit with less severity. Similarly, it is unlikely that the insertion location of the transgene is the cause of heart failure in TG-NS mice. First, two mutant TG-NS lines developed the same cardiac phenotype as TG-NSL12, but two TG-WT lines (L5 and L10) did not show signs of heart failure. Furthermore, two transgenic lines (unrelated to this study) that overexpress another *SCN5A* mutation (R1193Q) did not show the heart failure phenotype (data not shown). Taken together, the results on these multiple transgenic lines support the interpretation that it is the N1325S mutation, rather than the overexpression of *SCN5A* or the insertion location of the transgene in the genome, which causes contractile dysfunction.

Previously, we reported that in an LQTS family with the N1325S mutation, one of the three patients with echocardiographic data available clearly developed DCM [3]. Furthermore, in an LQTS family with the *SCN5A* mutation E1784K, the autopsy report on the proband (who died suddenly at age 31) revealed DCM [12]. Recently, Shi et al. reported that two mutation carriers in an LQT3 family with mutation delQKP 1507–1509 in *SCN5A* showed features of DCM [13]. The results with transgenic mice in this study substantiate the human studies and clearly indicate that there may be a potential risk of DCM associated with LQT3. However, it is important to note that the severity of contractile dysfunction seems to vary from one mouse to another. In humans, three patients in the LQTS family with the N1325S mutation had echocardiographic examinations, and one of them showed DCM. In mice, 50% of TG-NSL12 mice (3 of 6 mice) and 30% of TG-NSL3 mice (3 of 9 mice) showed typical features of DCM by both echocardiographic and histological examinations.

Several mutations in *SCN5A* have been reported to be associated with DCM, for example, heterozygous missense mutations D1275N, T220I, R814W and D1595H and one truncation mutation (2550–2551 ins TG) [14,15]. Compound heterozygous mutations W156X and R225W in *SCN5A* were associated with DCM, severe cardiac conduction disturbances and degenerative changes in the conduction system, and irregular wide complex tachycardia [16]. When expressed in *Xenopus* oocytes, mutant channels with W156X did not produce any current and those with R225W showed severely reduced sodium currents and abnormal gating. Three other mutations, D1275N, R814W and D1595H, were also functionally characterized. When expressed in *Xenopus* oocytes, mutation D1275N shifted the voltage dependence of activation to more depolarized voltages [17]. Mutations R814W and D1595H were studied in HEK293 cells [18]. D1595H impaired fast inactivation by slowing entry into the inactivated state, whereas R814W increased channel opening at hyperpolarized voltages. Interestingly, mutant R814W channels showed an increased late window current, a similar characteristic shared by mutation N1325S under the current study. These studies suggest that *SCN5A* mutations associated with DCM act by a diverse array of mechanisms. Curiously, different from the patients with mutation N1325S, the single patient with mutation R814W exhibited dilated cardiomyopathy, atrial fibrillation, and non-sustained ventricular tachycardia, but not LQTS associated with late sodium currents.

Multiple studies examined the link between prolonged QTc and heart failure in human patients. Davey et al. showed that the resting QTc was significantly longer in heart failure patients (470 ± 10 ms) than age-matched controls with normal left ventricular structure and

Please cite this article as: Zhang T, et al, LQTS mutation N1325S in cardiac sodium channel gene *SCN5A* causes cardiomyocyte apoptosis, cardiac fibrosis and contractile dysfunction in mice, Int J Cardiol (2009), doi:10.1016/j.ijcard.2009.08.047

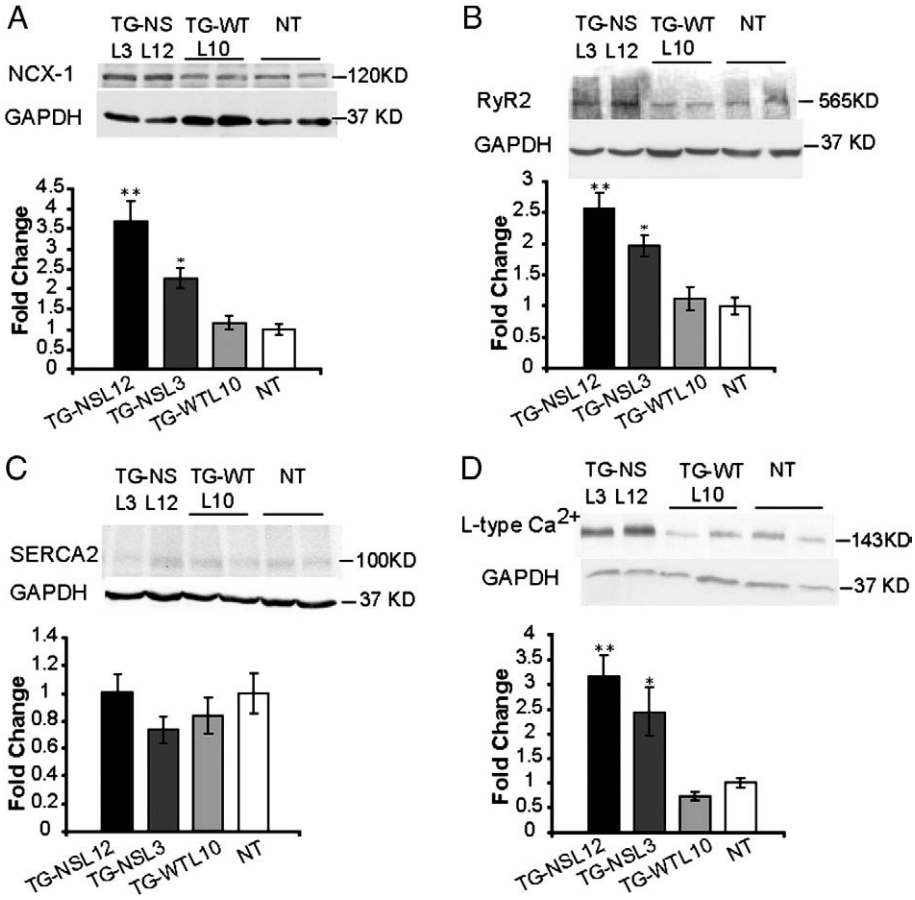

Fig. 6. Expression of NCX-1 (A), RyR2 (B), SERCA2 (C) and L-type Ca^{2+} channel (D) in hearts from TG-NS and NT mice at 3–5 months of age. Representative Western blots are shown at left panels and summarized data for the Western blot densitometrical analysis are at right panels. Cardiac expression of NCX-1 (A), RyR2 (B) and L-type Ca^{2+} (D) was significantly increased in TG-NSL3 and TGs-NSL12 mice, but not in TG-WTL10 mice or NT mice. Expression of SERCA2 (C) was not significantly different amongst the four groups of mice. (TG-NSL12 and TG-NSL3, $n=7$, respectively; TG-WTL10 and NT, $n=8$, respectively). $^{**}P<0.001$; $^{*}P<0.005$.

function (421 ± 6 ms) [19]. Among HF patients, 43%–72% of them showed prolonged QTc of >440 ms. VT, VF, and sudden death are also commonly documented in more than 50% patients with HF [20–22]. These important observations associated with heart failure were all captured in the TG-NS mice under this study. Therefore, TG-NS mice may serve as an animal model for investigating the pathogenic mechanisms of QT prolongation and ventricular arrhythmias associated with HF.

Our results suggest that cardiomyocyte apoptosis may be a cause of DCM in TG-NS mice. Consistent with this, cardiomyocyte apoptosis was shown to be the cause of contractile dysfunction in a transgenic mouse model, and its inhibition by caspase inhibitors improved LV function [7]. Cardiomyocyte apoptosis may also be a cause of ventricular arrhythmias in TG-NS mice. Apoptosis may lead to cardiac fibrosis, which then serves as a substrate for reentry arrhythmias detected in TG-NS mice. Although the detailed mechanism for apoptosis in TG-NS hearts is not known, activation of caspases 3 and 9, but not caspase-8, suggests that cardiomyocyte apoptosis in these mice is via the mitochondrial apoptotic pathway. An extensive microarray study revealed that expression of STAT1 was markedly increased in TG-NS hearts [23] and such an increase may contribute to increased cardiomyocyte apoptosis [24]. Furthermore, we showed that compared to TG-WTL10 mice, expression of L-type Ca^{2+} channel, RYR2, and NCX was increased in TG-NS mice (Fig. 5), which may be associated with abnormal Ca^{2+} homeostasis. Increased expression of the L-type Ca^{2+} channel on the cell surface and the calcium release channel RYR2 on sarcoplasmic reticulum membranes may increase the intracellular calcium concentration. Increased NCX expression in the context of increased late sodium current generated by mutation N1325S may increase the reverse mode activity of NCX, resulting in the increased intracellular calcium concentration. Aberrant Ca^{2+} homeostasis was linked to apoptosis and activation of caspases [25]. Future studies are needed to distinguish whether STAT1 overexpression or Ca^{2+} abnormalities are major causes of apoptosis in TG-NS hearts.

Although we cannot exclude the potential contribution of incessant tachyarrhythmias to the development of contractile dysfunction in TG-NS mice, we are not able to establish any association between the developments of these two disorders based on our data. We could detect both arrhythmias and contractile dysfunction in as early as 3 month old TG-NS mice and we have not observed any age preference to the onset of arrhythmias over contractile dysfunction. Therefore, the possibility exists that mutation N1325S could lead to the development of both incessant tachyarrhythmias and contractile dysfunction in parallel. However, tachycardia in TG-NSL12 mice could significantly contribute to the further development of contractile dysfunction, which can be investigated in the future by potential prevention of the phenotype by long-term application of beta blockers.

In summary, our results provide convincing evidence that cardiac structural abnormalities and contractile dysfunction can arise from transgenic overexpression of a congenital LQT3 mutation, N1325S, in *SCN5A*, which validates our earlier finding of an association of DCM with one N1325S carrier in humans. Overexpression of N1325S was associated with cardiomyocyte apoptosis and cardiac fibrosis, which could be contributing factors to contractile dysfunction. We postulate that expression remodeling of key cardiac proteins, including Ca^{2+} handling proteins or STAT1, leads to activation of caspases 3 and 9,

Please cite this article as: Zhang T, et al, LQTS mutation N1325S in cardiac sodium channel gene *SCN5A* causes cardiomyocyte apoptosis, cardiac fibrosis and contractile dysfunction in mice, Int J Cardiol (2009), doi:10.1016/j.ijcard.2009.08.047

which promotes cardiomyocyte apoptosis, resulting in contractile dysfunction. Furthermore, our results suggest that overexpression of an *SCN5A* mutation not only increases the occurrence of arrhythmias and sudden death, but also increases the risk for development of cardiac pump failure. Although heart failure can arise from a myriad of etiologies, the TG-NS mice with mutation N1325S should serve as an interesting model for studying the molecular mechanisms that underlie arrhythmias and progressive cardiac dysfunction and the development of heart failure.

Acknowledgements

We thank Drs. Judy Drazba and Peterson John for their help with image analysis. This work was supported by NIH/NHLBI grant R01 HL066251 (QW), an American Heart Association Postdoctoral Fellowship (0525523B, SLY), the National Basic Research Program of China (973 Program No. 2007CB512000) and an American Heart Association Established Investigator Award (0440157N) (QKW).

The authors of this manuscript have certified that they comply with the Principles of Ethical Publishing in the International Journal of Cardiology [26].

References

[1] Wang Q, Shen J, Li Z, Timothy K, Vincent GM, Priori SG, et al. Cardiac sodium channel mutations in patients with long QT syndrome, an inherited cardiac arrhythmia. Hum Mol Genet 1995;4:1603–7.
[2] Wang Q, Shen J, Splawski I, Atkinson D, Li Z, Robinson JL, et al. SCN5A mutations associated with an inherited cardiac arrhythmia, long QT syndrome. Cell 1995;80:805–11.
[3] Yong SL, Ni Y, Zhang T, Tester DJ, Ackerman MJ, Wang QK. Characterization of the cardiac sodium channel SCN5A mutation, N1325S, in single murine ventricular myocytes. Biochem Biophys Res Commun 2007;352:378–83.
[4] Tian XL, Yong SL, Wan X, Wu L, Chung MK, Tchou PJ, et al. Mechanisms by which SCN5A mutation N1325S causes cardiac arrhythmias and sudden death in vivo. Cardiovasc Res 2004;61:256–67.
[5] Tian XL, Cheng Y, Zhang T, Liao ML, Yong SL, Wang QK. Optical mapping of ventricular arrhythmias in LQTS mice with SCN5A mutation N1325S. Biochem Biophys Res Commun 2007;352:879–83.
[6] Zhang T, Yong SL, Tian XL, Wang QK. Cardiac-specific overexpression of SCN5A gene leads to shorter P wave duration and PR interval in transgenic mice. Biochem Biophys Res Commun 2007;355:444–50.
[7] Hayakawa Y, Chandra M, Miao W, Shirani J, Brown JH, Dorn 2nd GW, et al. Inhibition of cardiac myocyte apoptosis improves cardiac function and abolishes mortality in the peripartum cardiomyopathy of Galpha(q) transgenic mice. Circulation 2003;108:3036–41.
[8] Popovic ZB, Richards KE, Greenberg NL, Rovner A, Drinko J, Cheng Y, et al. Scaling of diastolic intraventricular pressure gradients is related to filling time duration. Am J Physiol Heart Circ Physiol 2006;291:H762–9.
[9] Hirota H, Chen J, Betz UA, Rajewsky K, Gu Y, Ross Jr J, et al. Loss of a gp130 cardiac muscle cell survival pathway is a critical event in the onset of heart failure during biomechanical stress. Cell 1999;97:189–98.
[10] Kerr JF, Wyllie AH, Currie AR. Apoptosis: a basic biological phenomenon with wide-ranging implications in tissue kinetics. Br J Cancer 1972;26:239–57.
[11] Feng Q, Song W, Lu X, Hamilton JA, Lei M, Peng T, et al. Development of heart failure and congenital septal defects in mice lacking endothelial nitric oxide synthase. Circulation 2002;106:873–9.
[12] Zhang L, V. G., Wang Q, Etheridge S, Zhang XQ, Chen SH, Phetchamphone T, Muhlestein JB, Anderson JL, Type 3 long QT syndrome, dilated cardiomyopathy, conduction abnormalities and Brugada syndrome variants in a large Caucasian kindred. Heart Rhythm 2008. 5: Supplementary S400.
[13] Shi R, Zhang Y, Yang C, Huang C, Zhou X, Qiang H, et al. The cardiac sodium channel mutation delQKP 1507–1509 is associated with the expanding phenotypic spectrum of LQT3, conduction disorder, dilated cardiomyopathy, and high incidence of youth sudden death. Europace 2008;10:1329–35.
[14] McNair WP, Ku L, Taylor MR, Fain PR, Dao D, et al. SCN5A mutation associated with dilated cardiomyopathy, conduction disorder, and arrhythmia. Circulation 2004;110:2163–7.
[15] Olson TM, Michels VV, Ballew JD, Reyna SP, Karst ML, Herron KJ, et al. Sodium channel mutations and susceptibility to heart failure and atrial fibrillation. Jama 2005;293:447–54.
[16] Bezzina CR, Rook MB, Groenewegen WA, Herfst LJ, van der Wal AC, Lam J, et al. Compound heterozygosity for mutations (W156X and R225W) in SCN5A associated with severe cardiac conduction disturbances and degenerative changes in the conduction system. Circ Res 2003;92:159–68.
[17] Groenewegen WA, Firouzi M, Bezzina CR, Vliex S, van Langen IM, Sandkuijl L, et al. A cardiac sodium channel mutation cosegregates with a rare connexin40 genotype in familial atrial standstill. Circ Res 2003;92:14–22.
[18] Nguyen TP, Wang DW, Rhodes TH, George Jr AL. Divergent biophysical defects caused by mutant sodium channels in dilated cardiomyopathy with arrhythmia. Circ Res 2008;102:364–71.
[19] Davey PP, Barlow C, Hart G. Prolongation of the QT interval in heart failure occurs at low but not at high heart rates. Clin Sci (Lond) 2000;98:603–10.
[20] Janse MJ. Electrophysiological changes in heart failure and their relationship to arrhythmogenesis. Cardiovasc Res 2004;61:208–17.
[21] Singh SN, Carson PE, Fisher SG. Nonsustained ventricular tachycardia in severe heart failure. Circulation 1997;96:3794–5.
[22] Vrtovec B, Ryazdanbakhsh AP, Pintar T, Collard CD, Gregoric ID, Radovancevic B. QTc interval prolongation predicts postoperative mortality in heart failure patients undergoing surgical revascularization. Tex Heart Inst J 2006;33:3–8.
[23] Wu L, Archacki SR, Zhang T, Wang QK. Induction of high STAT1 expression in transgenic mice with LQTS and heart failure. Biochem Biophys Res Commun 2007;358:449–54.
[24] Stephanou A, Brar BK, Scarabelli TM, Jonassen AK, Yellon DM, Marber MS, et al. Ischemia-induced STAT-1 expression and activation play a critical role in cardiomyocyte apoptosis. J Biol Chem 2000;275:10002–8.
[25] Orrenius S, Zhivotovsky B, Nicotera P. Regulation of cell death: the calcium-apoptosis link. Nat Rev Mol Cell Biol 2003;4:552–65.
[26] Coats AJ. Ethical authorship and publishing. Int J Cardiol 2009;131:149–50.

Please cite this article as: Zhang T, et al, LQTS mutation N1325S in cardiac sodium channel gene *SCN5A* causes cardiomyocyte apoptosis, cardiac fibrosis and contractile dysfunction in mice, Int J Cardiol (2009), doi:10.1016/j.ijcard.2009.08.047